Strain-level differences in gut microbiome composition determine fecal IgA levels and are modifiable by gut microbiota manipulation

Chao Yang,[1,2] Ilaria Mogno,[1,2] Eduardo J. Contijoch,[1,2] Joshua N. Borgerding,[1] Varun Aggarwala,[1,2] Zhihua Li,[2] Emilie K. Grasset,[1,6] Drew S. Helmus[3], Marla C. Dubinsky[3], Saurabh Mehandru,[1] Andrea Cerutti,[1,4,5] and Jeremiah J. Faith[1,2,]*

[1]Precision Immunology Institute, Icahn School of Medicine at Mount Sinai, New York, NY 10029, USA

[2]Institute for Genomics and Multiscale Biology, Icahn School of Medicine at Mount Sinai, New York, NY 10029, USA

[3]Pediatric Gastroenterology and Hepatology, Department of Pediatrics, Susan and Leonard Feinstein IBD Clinical Center, Icahn School of Medicine at Mount Sinai, New York, NY 10029, USA

[4]Program for Inflammatory and Cardiovascular Disorders, Institut Hospital del Mar d'Investigacions Mediques (IMIM), Barcelona 08003, Spain

[5]Catalan Institute for Advanced Studies (ICREA), Barcelona 08003, Spain

[6]Department of Medicine, Center for Molecular Medicine, Karolinska Institutet, Karolinska University Hospital, SE-171 77 Stockholm, Sweden

*Correspondence: jeremiah.faith@mssm.edu (J.J.F.)

Keywords

Gut microbiota, Immunoglobulin A, *Bacteroides ovatus*, Fecal Microbiota Transplantation, Immune modulation

Abstract

Fecal IgA production depends on colonization by a gut microbiota. However, the bacterial strains that drive gut IgA production remain largely unknown. By accessing the IgA-inducing capacity of a diverse set of human gut microbial strains, we identified *Bacteroides ovatus* as the species that best induced gut IgA production. However, this induction varied biomodally across different *B. ovatus* strains. The high IgA-inducing *B. ovatus* strains preferentially elicited more IgA production in the large intestine through both T-cell-dependent and T-cell-independent B cell-activation pathways. Remarkably, a low-IgA phenotype in mice could be robustly and consistently converted into a high-IgA phenotype by transplanting a multiplex cocktail of high IgA-inducing *B. ovatus* strains but not individual ones. Thus, microbial strain specificity is essential for the optimal induction of high-IgA responses in the gut. Our results highlight the critical importance of microbial strains in driving phenotype variation in the mucosal immune system and provide a strategy to robustly modify a gut immune phenotype, including IgA production.

42 **Introduction**

43 Immunoglobulin A (IgA) is the most abundant mucosal antibody and plays an essential role in
44 maintaining gut homeostasis as well as other physiological processes[1-3]. Secretory IgA, for
45 example, can limit the access of bacteria and bacteria-derived toxins to intestinal epithelial
46 cells[4,5], facilitate the clearance of bacteria that have breached the mucosal barrier[6-8] and
47 regulate the colonization of bacteria in the mucosal lining[9,10]. In addition, IgA can also bind
48 disease-associated gut microbiota[11-13]. Conversely, the gut microbiota and its metabolites drive
49 the production of IgA as germ-free (GF) mice have an almost undetectable level of fecal IgA[14].
50 Upon bacteria colonization, even with a single bacterial strain[15-17], B cells undergo class-switch
51 to IgA^+ cells in gut-associated lymphoid tissues (GALT), which include Peyer's patches (PP),
52 isolated lymphoid follicles (ILF) and mesenteric lymph nodes (MLN), and in the gut lamina
53 propria (LP)[8,18]. Much of the intestinal IgA is bacteria-specific[15,16,19], and the B-cell repertoire is
54 highly influenced by the microbiota composition[20]. To date, a few murine derived bacterial
55 species have been identified as being able to enhance or reduce intestinal IgA production[21-25].
56 However, key questions regarding the impact of microbiota in this process remain largely
57 unanswered including the importance of colonization order, the contribution of individual
58 bacterial species versus that of microbial communities, the potential to modulate IgA production
59 by altering gut microbiota composition with commensal organisms, and the role of each
60 microbial species in the development of IgA^+ B cells in specific tissues[8,26].

61 Apart from IgA-secreting cells, the gut microbiota has the capacity to influence numerous
62 other immune cell populations including colonic regulatory T cells[27-29], IL-17 producing T helper
63 cells[30], and macrophages[31]. Importantly, many of these responses seem to be bacterial strain-
64 specific as communities with comparable species composition can drive gut immune responses
65 characterized by largely different cell compositions[32]. These discoveries indicate that
66 manipulation of the gut microbiota, with appropriate bacterial strains, represents a potential
67 therapeutic pathway for the treatment of diseases including inflammatory bowel disease,

68 rheumatoid arthritis and multiple sclerosis through shaping the host immune system[33]. Although
69 the studies of microbiota-based therapeutics (MT) and fecal microbiota transplantation (FMT)
70 have heavily focused on the engraftment of the transmitted microbiota and its influence on the
71 composition of the recipient microbiota[34-37], the clinical application of microbiota manipulation as
72 an immunomodulatory strategy will require combinations of bacterial strains optimized for the
73 induction of specific immune phenotypes that are robust to the interpersonal variation in the pre-
74 existing microbiota of each recipient.

75 Here we demonstrate that, upon transfer into GF mice, human isolates of the *Bacteroides*
76 *ovatus* species, one of the most common human gut commensals, are uniquely capable of
77 inducing high mucosal IgA production compared with other common gut commensal species.
78 This IgA-inducing capacity, however, was restricted to specific strains of *B. ovatus* that
79 preferentially led to IgA production in the large intestine through both T-cell-dependent (TD) and
80 T-cell-independent (TI) B cell-activation pathways. While no individual bacterial strain functioned
81 as an effective enhancer of gut IgA production, we found that cocktails of these high IgA-
82 inducing (IgA^{high}) strains could serve as effective immunomodulators, that elicited higher fecal
83 IgA levels upon administration to animals harboring a pre-existing microbiota with low IgA-
84 inducing potential (IgA^{low}). Our work demonstrates the importance of strain-level variation in gut
85 microbiota composition on mucosal immune responses. It also supports the potential utility of
86 cultured multi-bacterial effector strain cocktails as a strategy to overcome phenotype transfer
87 resistance in microbiota-based immunomodulation[38].
88

Results

B. ovatus elicits robust gut IgA production

To determine if individual gut bacterial species have a distinct IgA-inducing potential, we monocolonized GF C57BL/6 mice with one of eight different human gut commensal bacteria (Supplementary Table 1) with representatives from the most prominent phyla of the human gut including Firmicutes, Bacteroidetes, Actinobacteria and Proteobacteria[39,40]. After three weeks of colonization to allow optimal steady-state gut IgA secretion (Supplementary Fig. 1a), we measured serum and fecal IgA levels in each group of gnotobiotic mice[16]. Although all tested species significantly increased IgA level relative to control GF mice, *B. ovatus* monocolonized mice secreted significantly more IgA in their feces compared with mice colonized with any of the other seven human gut bacteria (Fig. 1a; $p < 0.001$). Most species also increased serum IgA (Supplementary Fig. 1b). However, consistent with previous reports[18], fecal IgA and serum IgA levels in these mice did not correlate significantly (Supplementary Fig. 1c; $R^2 = 0.226$; $p = 0.196$). GF mice colonized with the cocktail of all eight bacterial species yielded as much fecal and serum IgA as mice monocolonized with *B. ovatus*.

To address if the order of bacterial colonization could influence fecal IgA secretion, GF mice were sequentially colonized every three weeks with individual species or small cocktails of the same eight bacterial species. We first assayed fecal IgA level in mice sequentially colonized with low IgA inducers (e.g. *E. coli*) to high IgA inducers (e.g. *B. ovatus*). Fecal IgA increased gradually with the colonization of additional bacterial species. However, the more striking (>2-fold) increase in IgA occurred after colonization with *B. ovatus* (Fig. 1b). Metagenomic sequencing of fecal microbiota in these mice revealed gut colonization by each bacterial species, albeit with different proportions (Fig. 1c). We then reversed the order of colonization from high IgA inducers (e.g. *B. ovatus*) to low IgA inducers (Fig. 1d). Once again, *B. ovatus* elicited the largest increase of fecal IgA production, while the other species led to smaller increases (Fig. 1e). Remarkably, the relative abundance of each organism at the end of the

115 colonization was very similar, regardless of the order of colonization (Fig. 1c,e). These results
116 demonstrate that *B. ovatus* is a uniquely potent gut IgA inducer and that the species
117 composition of the gut microbiota impacts IgA production more than the order of bacterial
118 colonization.

119 To test the role of bacterial viability in the induction of gut IgA by *B. ovatus*[15,41,42], GF mice
120 were administered heat-killed *B. ovatus* or *B. ovatus* metabolites (i.e. filtered growth medium
121 from stationary phase of *B. ovatus* cultures) for three weeks. Neither approach was capable of
122 enhancing fecal IgA above the level detected in GF mice (Supplementary Fig. 1d). To ensure
123 the above result was not due to the underdeveloped mucosal immune system of GF mice, we
124 performed similar experiments by first colonizing GF mice with *E. coli* for three weeks and
125 subsequently treated these mice with heat-killed *B. ovatus* for an additional three weeks. Again,
126 we found no significant fecal IgA increase (Supplementary Fig. 1d). Thus, neither dead *B.*
127 *ovatus* nor its metabolites triggered efficient gut IgA responses in the murine intestine. All
128 together, live *B. ovatus* species elicited more gut IgA production than other tested gut
129 commensal bacterial species in GF mice.

130

131 ***B. ovatus*-driven gut IgA production is strain-specific**

132 Given the remarkable microbial strain variation across individuals[43-46], we wondered whether all
133 *B. ovatus* strains within this common bacterial species induced comparably high fecal IgA. GF
134 mice monocolonized for three weeks with one of 19 *B. ovatus* strains isolated from 19 different
135 individuals (Supplementary Table 2) showed a strain-specific gut IgA response (Fig. 1f; $p <$
136 0.0001 one-way ANOVA). In contrast to the large variability of fecal IgA levels, serum IgA levels
137 were comparable across mice monocolonized with different *B. ovatus* strains (Supplementary
138 Fig. 1e). Similarly, the colonization density was also comparable across mice harboring different
139 *B. ovatus* strains (Supplementary Fig. 1f). This observation suggests that the global density of
140 each individual strain was not implicated in the genesis of strain-specific differences of gut IgA

141 responses. Of note, the distribution pattern of IgA induction across multiple *B. ovatus* strains
142 was bimodal (Supplementary Fig. 1g; p = 0.0481 Hartigans' Dip Test), allowing these strains to
143 be categorized as IgA^{high} or IgA^{low}. The genomic similarity of *B. ovatus* strains was not a
144 significant predictor of their IgA^{high} and IgA^{low} properties (Fig. 1g and Supplementary Table 3),
145 which suggests that their distinct IgA-inducing function is shared amongst the species rather
146 than representing an evolutionarily distinct group within the species.

147 To rule out a bias in our preliminary screen for IgA^{low} strains within the *Bacteroides* genus,
148 we assayed whether additional strains could induce high fecal IgA (Fig. 1a). We found no strain-
149 specific differences in fecal IgA induction when GF mice were monocolonized with three distinct
150 strains of *B. caccae*, *B. thetaiotaomicron* and *B. vulgatus* (Supplementary Fig. 1h). The IgA-
151 inducing function of additional common species from the order Bacteroidales, including
152 *Parabacteroides johnsonii*, *Bacteroides intestinalis* and *Bacteroides fragilis,* were tested but also
153 induced much less gut IgA than *B. ovatus* (Supplementary Fig. 1h). These results indicate that
154 the high IgA-inducing ability of *B. ovatus* is unique to this gut bacterial species and only to a
155 subset of strains.

156 To examine the influence of *B. ovatus* strain variation on host fecal IgA production in the
157 context of more complex gut microbiotas, we colonized GF mice with one of the seven
158 microbiota arrayed culture collections originally isolated from different human donors with each
159 collection consisting of 15-20 unique species[32]. The arrayed culture collections were assembled
160 to reconstitute a donor microbiota each containing a unique *B. ovatus* strain, which was already
161 functionally tested by earlier monocolonization (Fig. 1f). We observed a significant positive
162 correlation between the fecal IgA concentrations induced by an individual *B. ovatus* strain and
163 the fecal IgA concentrations elicited by a culture collection representing the entire *B. ovatus*-
164 containing microbiota from the same donor (Fig. 1h; R^2 = 0.859, p = 0.0027). Again, these
165 results suggest that the *B. ovatus* strain composition is a major contributor of gut IgA responses
166 even when considered in the context of complex microbial communities.

167 Unlike inbred laboratory mice housed in a highly controlled environment, human beings,
168 with different genetic background, are exposed to more complex continuum of factors including
169 some that were demonstrated to affect fecal IgA production such as genetics and diet[47,48]. To
170 determine whether *B. ovatus* could drive robust gut IgA responses also in humans, we
171 measured the fecal concentration of IgA in multiple human donors and correlated this
172 concentration with that of fecal IgA generated by GF mice monocolonized with a *B. ovatus* strain
173 isolated from identical donors. Though no significant correlation was observed, there was a
174 clear trend towards a positive correlation even in an uncontrolled condition (Fig. 1i; $R^2 = 0.2071$,
175 $p = 0.0765$).

176 In total these results demonstrate that a subset of *B. ovatus* strains induce high fecal IgA
177 levels, which broadly influence the total fecal IgA output of the host even in the context of a
178 diverse gut microbiota.

179

180 **IgA^{high} *B. ovatus* strains induce more IgA production in the large intestine**

181 To interrogate the mechanisms underpinning gut IgA induction by different *B. ovatus* strains, GF
182 mice were colonized with a representative IgA^{high} or IgA^{low} strain (*B. ovatus* strain *E* and *Q,*
183 respectively). We quantified bacteria-bound IgA in the stool of mice. Monocolonization with the
184 IgA^{high} strain *E* not only induced more free fecal IgA but also more fecal bacteria-bound IgA than
185 the IgA^{low} strain *Q* did (52.9% vs. 21.0% IgA-coated *B. ovatus*) (Fig. 2a). In contrast, no
186 significant difference was observed in serum immunoglobulin isotypes (i.e. IgA, IgG1, IgG2a,
187 IgG2b, IgG3, IgM and IgE) in monocolonized mice harboring either *B. ovatus* strain *E* or *Q*
188 (Supplementary Fig. 1e, 2a).

189 Fecal IgA mostly derives from polymeric IgA released by IgA$^+$ plasma cells residing in the
190 intestinal LP and translocated to the gut lumen across epithelial cells via transcytosis[49]. This
191 process is mediated by a basolateral IgA (and IgM) transporter termed polymeric
192 immunoglobulin receptor (pIgR)[49]. Independent groups have reported that the expression of

193 pIgR by gut epithelial cells is influenced by bacteria stimulation both *in vivo* and *in vitro*[50,51]. To
194 determine if *B. ovatus* strain variation impacts fecal IgA level by modulating pIgR-mediated
195 transcytosis, we imaged the expression of pIgR by immunofluorescence staining in the small
196 intestine and the colon of mice colonized with either *B. ovatus* strain *E* (IgA^{high}) or *Q* (IgA^{low}).
197 However, no noticeable difference in pIgR expression was observed (Supplementary Fig. 2b).
198 To further interrogate the mechanism underpinning the increased fecal IgA in *B. ovatus* strain *E*
199 colonized mice, we then quantified, by histology and flow cytometry, IgA^+ B cells in both small
200 intestine and the colon. We found more IgA^+ B cells in the colonic LP of mice harboring *B.*
201 *ovatus* strain *E* compared to mice harboring strain *Q*, while no significant strain-specific
202 difference was observed in the small intestine (Fig. 2b,c). Although PPs and MLNs usually serve
203 as dominant IgA inductive sites[52,53], we did not observe a significant difference in IgA^+ B cells at
204 these sites by strain *E* or strain *Q* (Supplementary Fig. 3).

205 Given the preferential expansion of IgA^+ B cells in the colons of monocolonized mice
206 harboring *B. ovatus* strain *E*, we then explored whether luminal IgA levels would vary between
207 small and large intestinal regions. In the small intestine, we found that mice monocolonized with
208 *B. ovatus* strain *E* or strain *Q* had comparable luminal IgA levels (Fig. 2d). In contrast, mice
209 monocolonized with strain *E* had significantly more luminal IgA from cecum to distal colon than
210 those colonized with strain *Q* (Fig. 2d). Similar results were also observed across all tested
211 IgA^{high} and IgA^{low} *B. ovatus* strains (Supplementary Fig. 4). Thus, the IgA^{high} *B. ovatus* strains
212 induce more colonic IgA-secreting cells compared to IgA^{low} *B. ovatus* strains, which results in
213 the secretion of more IgA in the large intestinal lumen.

214 To determine if these observations were unique to GF C57BL/6 mice, we recapitulated our
215 monocolonization strategy in GF Swiss Webster mice and found that fecal IgA was largely
216 comparable in gnotobiotic C57BL/6 and Swiss Webster mice colonized with identical bacterial
217 strains (Supplementary Fig. 5a-d; $R^2 = 0.601$, $p = 0.0011$). Moreover, IgA^{high} strain colonized
218 gnotobiotic Swiss Webster mice also secreted more intraluminal IgA in the large intestine

219 compared with IgA^{low} strain colonized mice (Supplementary Fig. 5e). Thus, bacteria-induced gut
220 IgA production is similar across different host genetic backgrounds.
221
222 **_B. ovatus_ elicits gut IgA production via both TD and TI B cell-activation pathways**
223 Gut IgA responses occur through TD or TI B cell-activation pathways[52,54]. To determine the
224 influence of CD4^{+} T cells on the gut IgA production induced by *B. ovatus*, we depleted CD4^{+} T
225 cells in mice by injecting with an anti-CD4 antibody five days prior to and for three weeks after
226 monocolonization with *B. ovatus* strain *E* (Fig. 3a and Supplementary Fig. 6a-c). On day seven
227 post-colonization, fecal IgA increased in both T cell-depleted and T cell-sufficient gnotobiotic
228 mice, which suggests that CD4^{+} T cells are not a dominant factor in early stage IgA induction.
229 By day 14 post-colonization, control mice receiving an isotype-matched irrelevant antibody
230 generated significantly more fecal IgA than mice receiving anti-CD4 antibody (Fig. 3b). In
231 addition to reduced free IgA, *B. ovatus*-bound IgA also decreased in the stool of CD4^{+} T cell-
232 depleted mice (Fig. 3c). In both small intestine and the colon, the frequency of IgA^{+} B cells was
233 reduced by approximately 1/3 compared to that of IgA^{+} B cells being detected in the control
234 CD4^{+} T cell-sufficient mice (Fig. 3d and Supplementary Fig. 6d,e). In addition, these control
235 mice showed more intraluminal IgA than CD4^{+} T cell-depleted mice across the whole intestinal
236 tract (Fig. 3e).
237
238 **Multiplex cocktail of _B. ovatus_ strains robustly modify gut IgA production**
239 Given the potential of gut microbiota manipulation as a therapeutic, we next determined whether
240 the high-IgA phenotype could be transferred to mice harboring microbiotas that induce a low
241 level of fecal IgA. For this purpose, we recolonized GF C57BL/6 mice with either *B. ovatus*
242 strain *E* (IgA^{high}) or *Q* (IgA^{low}) for three weeks, followed by cohousing these mice for an
243 additional three weeks (Fig. 4a). After cohousing, mice monocolonized with *B. ovatus* strain *Q*
244 showed no significant change in fecal IgA. In contrast, mice colonized initially with *B. ovatus*

245 strain *E* had reduced fecal IgA, which raised the possibility that the low-IgA phenotype behaves
246 as a dominant character in the context of this simple bacterial community (Fig. 4b). Interestingly,
247 the IgA^{low} *B. ovatus* strain *Q* also dominated the relative abundance of the microbiota, as it
248 represented ~95% of the microbiota compared with ~5% of *B. ovatus* strain *E* (Fig. 4c). In an
249 attempt to overcome this resistance to transfer of the high-IgA phenotype to mice with low-IgA
250 phenotype, we performed a similar experiment but added three more IgA^{high} *B. ovatus* strains.
251 Under these conditions, the high-IgA phenotype was transfered to the cohoused mice initially
252 monocolonized with the IgA^{low} strain (Supplementary Fig. 7a). However, *B. ovatus* strain *Q* still
253 represented a substantial proportion (32.5 ~ 53.8%) of the relative abundance in this bacterial
254 community (Supplementary Fig. 7b). Thus, a multiplex cocktail of bacterial effector strains that
255 each individually can induce a specific phenotype provides a more robust strategy for
256 transferring a high-IgA phenotype.

257 Beyond cohousing, we further validated the above findings by transferring IgA^{high} strains
258 therapeutically by oral gavage. Consistent with the cohousing results, mice first colonized with
259 an IgA^{low} *B. ovatus* strain and then orally gavaged with an additional IgA^{high} strain did not alter
260 gut IgA secretion. In contrast, mice receiving a cocktail of four IgA^{high} *B. ovatus* strains (*B.*
261 *ovatus* 4M) produced significantly more fecal IgA (Fig. 4d and Supplementary Table 4).
262 Metagenomic sequencing results demonstrated that multiple *B. ovatus* strains colonized the
263 recipient mice (Fig. 4e). Of note, IgA^{low} *B. ovatus* strain *Q* still dominated the relative abundance
264 of the gut microbiota in individual strain transfers (Fig. 4e). IgA^{high} strains accounted for 44% of
265 the gut microbiota in the *B. ovatus* 4M transfer with each individual IgA^{high} strain having a
266 distinct relative abundance (Fig. 4e). Finally, we replicated these results in mice pre-colonized
267 with another IgA^{low} *B. ovatus* strain *R* (Supplementary Fig. 7c,d).

268 To validate these results in the setting of more complex gut microbiotas, we performed
269 similar experiments using either gnotobiotic mice colonized by a synthetic cocktail of diverse
270 bacterial species that included *B. ovatus* IgA^{low} strain *Q* (Supplementary Table 5) or gnotobiotic

271 mice colonized with arrayed culture collections established from donors harboring a functionally
272 validated IgA^{low} *B. ovatus* strain (Fig. 1h and Supplementary Table 6). As with simpler
273 communities, transfer of the high-IgA phenotype was robustly achieved with *B. ovatus* 4M or a
274 multiplex cocktail of eight IgA^{high} *B. ovatus* strains (*B. ovatus* 8M) (Supplementary Table 4) but
275 not by individual IgA^{high} *B. ovatus* strains (Fig. 4f and Supplementary Fig. 7e). Consistent with
276 our previous findings, IgA was elevated only in the large intestine (Fig. 4g and Supplementary
277 Fig. 7f). The relative proportions of each IgA^{high} strain and total relative abundance of all IgA^{high}
278 strains in the stool of multiplex bacterial cocktail recipient mice varied across recipient
279 microbiota communities (Fig. 4h,i and Supplementary Fig. 7g,h).

280 To further validate the IgA-inducing properties of our multiplex IgA^{high} *B. ovatus* cocktails,
281 we tested these cocktails in two additional gnotobiotic mouse models colonized by human
282 microbiota arrayed culture collections with low-IgA potential (Supplementary Table 6). Again, we
283 found that the multiplex IgA^{high} *B. ovatus* cocktails robustly increased fecal IgA (Supplementary
284 Fig. 8a-f). Across all of the tested *B. ovatus* 4M and *B. ovatus* 8M recipients, we did not find a
285 correlation between the total relative abundance of IgA^{high} strains and the fecal IgA levels, which
286 indicates that maximizing the total abundance of IgA^{high} *B. ovatus* strains does not necessarily
287 increase gut IgA production (Supplementary Fig 8g-i). In summary, our results demonstrate that
288 transfer of multiplex IgA^{high} *B. ovatus* strain cocktails, but not that of individual IgA^{high} strains,
289 consistently and robustly modulates the immune system (e.g. IgA phenotype) across several
290 complex pre-existing gut microbiota.
291

292 **Discussion**

293 Functional differences of pathogenic bacteria at the strain level have been intensively studied in
294 the past decades and are a fundamental component of infectious disease clinical practice. More
295 recently the functional impact of bacterial strain variation is becoming apparent in the context of
296 the protective or disease-enhancing properties of the commensal microbiota[11,12,32,55,56]. Here, we
297 identified that approximately half of the isolated strains from *B. ovatus* species, which is one of
298 the most common species of our gut commensal microbiota, drive increased IgA production in
299 the distal intestinal tract. Interestingly, we did not find that the variation in fecal IgA induced by
300 different *B. ovatus* strains was related to unique genetic lineages amongst strains or the density
301 of the bacteria in the feces. Through manipulation of the pre-existing gut microbiota
302 composition, we discovered that cocktails of IgA^{high} *B. ovatus* strains were more efficient than
303 individual IgA^{high} *B. ovatus* strains in converting mice with low gut IgA production into mice
304 producing large amounts of gut IgA.

305 IgA^{high} *B. ovatus* strains increased IgA production in distal but not proximal intestinal
306 segments by enhancing the ratio of IgA-secreting B cells. Remarkably, this induction was not
307 dominated by the migration of IgA^{+} B cells from canonical IgA inductive sites, as gnotobiotic
308 mice colonized with either IgA^{high} or IgA^{low} *B. ovatus* strains showed comparable IgA^{+} B cells in
309 PPs and MLNs. One possibility is that IgA^{high} *B. ovatus* strains locally elicit IgA production in the
310 large intestine including cecal patches, ILFs and LP[2,54,57]. Interestingly, mice harboring specific
311 *B. ovatus* strains showed no significant differences in the intestinal abundance of *B. ovatus*,
312 which further highlights the unique IgA-inducing properties of individual strains.

313 After IgA^{high} *B. ovatus* strain colonization, CD4^{+} T cell-depleted mice showed a reduced
314 ratio of IgA^{+} B cells in the gut, in turn leading to decreased luminal IgA along the entire intestinal
315 tract. Of note, both CD4^{+} T cell-sufficient and T cell-depleted mice produced comparable level of
316 gut IgA at the beginning post colonization, which suggests CD4^{+} T cells play less of a role
317 during the very early stage of IgA induction likely due to the dominance of the TI B cell-

318 activation pathway. Interestingly, a protein from the gut commensal *Lactobacillus rhamnosus*
319 was recently shown to locally elicit IgA production via gut epithelial cells[58]. Thus, further studies
320 will be needed to delineate the precise mechanisms whereby IgA^{high} *B. ovatus* strain colonized
321 mice generate gut IgA. Nevertheless, our study highlights the important contribution of T cells in
322 bacteria-mediated IgA production, especially in the large intestine[59,60].

323 FMT-based manipulation of the gut microbiota has a high success rate in the treatment of
324 recurrent *C. difficile* infection[61]. However, its success in other indications, such as ulcerative
325 colitis, is more limited[62,63]. Although improving bacteria engraftment remains a key therapeutic
326 goal of microbiota manipulation[62-64], identifying new strategies that optimize the transfer of a
327 specific immune phenotype constitutes a therapeutic goal with a potentially larger range of
328 applications. Using IgA induction as an example of immunomodulatory phenotype transfer, our
329 data showed that multiplex bacterial cocktails of IgA^{high} *B. ovatus* strains elicited a more robust
330 phenotype transfer than any individual strain, even in mice with complex gut ecosystem. This
331 multiplex effector strain cocktail strategy was robust across multiple recipients, who had low-IgA
332 phenotype and pre-colonized with different microbiotas, and could represent an effective
333 approach to therapeutically modify gut immune parameters in addition to IgA. Of note, across
334 the tested inductions of IgA via gut microbiota manipulation with IgA^{high} *B. ovatus* strains, we
335 found that no single strain consistently dominated over the others. Thus, multiplex bacterial
336 cocktails do not appear to have “super strains” with dominant IgA-inducing function. Rather, the
337 combination of multiple IgA^{high} effector strains in these cocktails has an IgA-inducing potential
338 superior to that of any individual strain. Intriguingly, the relative abundance of total *B. ovatus*
339 species remained largely stable even after the introduction of one to eight new strains
340 suggesting that these new strains largely share the same ecological niches as that occupied by
341 the pre-existing *B. ovatus*.

342 In summary, our results highlight the importance of bacterial strain variation on the IgA-
343 inducing potential of the gut microbiota. In addition, we also identify a new strategy (e.g.

344 multiplex bacterial strain cocktail) for the exploitation of strain variation in the development of
345 robust microbiota-based immunomodulation therapeutic strategies.
346

347 ## Methods

348 ### Mice

349 Germ-free C57BL/6 and Swiss Webster mice were bred and maintained in flexible film
350 gnotobiotic isolators (Class Biologically Clean, Ltd.). All mice were group housed with a 12-hour
351 light/dark cycle and allowed *ad libitum* access to diet and water. All animal studies were carried
352 out in accordance with protocols approved by the Institutional Animal Care and Use Committee
353 (IACUC) in Icahn School of Medicine at Mount Sinai.

354

355 ### Colonization of germ-free mice with cultured bacteria

356 Germ-free mice (~8 weeks old) were colonized 200-µl aliquot of bacteria suspension via oral
357 gavage. Colonized mice were housed in flexible film vinyl isolators or in filter top cages using
358 previously described techniques[43].

359

360 ### Growth and isolation of bacterial strains

361 All bacterial strains were obtained from previously banked stool, public culture repositories or
362 human gut microbiota arrayed culture collections[27]. All bacterial strains isolated for this study
363 were isolated from deidentified stool samples from individuals under a Mount Sinai IRB
364 approved protocol (IRB-16-00008). All bacteria apart from *E. coli* were grown under anaerobic
365 condition at 37°C in Brain Heart Infusion (BHI) medium supplemented with 0.5% yeast extract
366 (Difco Laboratories), 0.4% monosaccharide mixture, 0.3% disaccharide mixture, L-cysteine (0.5
367 mg/ml; Sigma-Aldrich), malic acid (1 mg/ml; Sigma-Aldrich) and 5 µg/ml hemin. *E. coli* was
368 cultured in LB Broth Miller (EMD Chemicals, Inc.) under aerobic condition at 37°C.

369

370 ### Quantification of immunoglobulins by ELISA

371 Total fecal and serum IgA were measured by sandwich ELISA. For total IgA detection, ELISA
372 plates (Corning 3690) were coated with 1 µg/ml goat anti-mouse IgA (SouthernBiotech, AL)

373 capture antibody overnight at 4°C. Plates were washed and blocked with 1% BSA in PBS for 2 h
374 at room temperature. Diluted samples and standards were added and incubated overnight at
375 4°C. Captured IgA was detected by horseradish peroxidase (HRP)-conjugated goat anti-mouse
376 IgA antibody (Sigma-Aldrich). ELISA plates were developed by TMB microwell peroxidase
377 substrate (KPL, Inc.) and quenched by 1 M H_2SO_4. Colorimetric reaction was measured at OD =
378 450 nm by a Synergy™ HTX Multi-Mode Microplate Reader (BioTek Instruments, Inc.). Other
379 serum immunoglobulins (IgG1, IgG2a, IgG2b, IgG3, IgM and IgE) were also detected using
380 sandwich ELISA with the following capture and detection antibody pairs (all the following
381 antibodies were purchased from SouthernBiotech, AL): goat anti-mouse IgG1, goat anti-mouse
382 IgG2a, goat anti-mouse IgG2b, goat anti-mouse IgG3, rat anti-mouse IgE, rat anti-mouse IgM,
383 goat anti-mouse IgG-HRP, goat anti-mouse IgE-HRP and goat anti-mouse IgM-HRP.
384 Corresponding mouse immunoglobulin isotypes were used as standards.
385

386 **Depletion of $CD4^+$ T Cells in germ-free mice**

387 *In vivo* depletion of $CD4^+$ T cells was performed as described[65]. Briefly, gnotobiotic mice (8
388 weeks old) were first injected intraperitoneally (i.p.) with anti-mouse CD4 monoclonal antibody
389 (Bio X Cell, clone GK1.5) or matched isotype control (Bio X Cell, clone LTF-2) at 0.5
390 mg/day/mouse for 3 consecutive days. Then the injection was performed every 3 days for a
391 period of 3 weeks. Five days after the first antibody injection, mice were inoculated via oral
392 gavage with *B. ovatus* strain *E*. Efficacy of T cell depletion was evaluated by flow cytometry.
393

394 **Lymphocyte isolation from tissues**

395 To isolate mononuclear cells from Peyer's patches (PPs), PPs were excised from mouse small
396 intestines and incubated in dissociation buffer, containing Hank's Balanced Salt Solution
397 (HBSS) without Ca^{2+} and Mg^{2+} (GIBCO), 10% fetal bovine serum (FBS), 5 mM EDTA and 15
398 mM HEPES, at 37°C for 30 min. Later, tissues were mechanically separated by pushing them

399 through a 70 μm strainer into Iscove's Modified Dulbecco's Medium (IMDM) supplemented with
400 2% FBS. Filtered cells were spun down, washed and resuspended in IMDM/2%FBS. Lamina
401 propria lymphocytes were isolated as described[27]. Briefly, small intestines and colons were
402 excised, followed by removing visceral fat and intestinal contents. Tissues were opened
403 longitudinally, washed twice in HBSS and incubated in dissociation buffer for 30 min at 37°C
404 with mild agitation to remove epithelium and intraepithelial lymphocytes. Tissues were then
405 washed three times in ice cold HBSS, cut into ~2 cm pieces and digested with collagenase
406 (Sigma-Aldrich), DNase I (Sigma-Aldrich) and dispase I (Corning). Cell suspensions were
407 filtered through 70 μm cell strainers, washed three times, and resuspended in IMDM/2%FBS.
408 Mesenteric lymph nodes were separated from mesenteric fat and dissociated in IMDM/2%FBS
409 by physically pressing the tissues between the frosted portions of two glass microscope slides.
410 The cell suspension was filtered through a 70 μm cell strainer, washed three times and
411 resuspended in IMDM/2%FBS
412
413 **Detection of IgA-coated bacteria in feces**
414 IgA-coated fecal bacteria were measured by flow cytometry as previously described[12,13]. Briefly,
415 mouse fecal pellets, stored at -80°C freezer after collection, were dissolved in PBS to a final
416 concentration of 100 milligram per milliliter PBS by weight, thawed at room temperature,
417 homogenized in vortex mixer and centrifuged at 4°C to remove large particles. The supernatant
418 was passed through a 40 μm sterile nylon filter and 50 μl aliquot of the bacteria suspension was
419 collected for staining. Bacteria were pelleted by centrifugation and washed in 1ml of
420 PBS/1%BSA/2mM EDTA for 3 times. Non-specific binding sites were first blocked with 50 μl
421 PBS/1%BSA/20% rat serum for 20 min at 4°C. Bacteria were then stained with 50 μl
422 of PBS/1%BSA/2mM EDTA buffer containing 1:100 dilution of monoclonal rat anti-mouse IgA
423 antibody (eBioscience, clone mA-6E1) for 30 min at 4°C. After washing 3 times, bacterial pellets
424 were resuspended in PBS containing SYBR Green I (1:100,000 dilution; Invitrogen). Samples

425 were run through a BD LSR Fortessa™ cell analyzer and further analyzed by FlowJo software
426 (Tree Star, Inc.). Only SYBR positive events were regarded as bacteria and gated for further
427 quantification of IgA-coated bacteria (Supplementary Fig. 9).
428
429 **Flow cytometry analysis and antibodies**
430 Isolated mononuclear cells were washed in PBS and incubated with Zombie Aqua™ dye
431 (BioLegend) to distinguish live and dead cells. Before surface staining, non-specific binding of
432 immunoglobulin to Fc receptors was blocked by anti-mouse CD16/32 antibody (BD
433 Biosciences). Cells were stained in FACS buffer (PBS without Ca^{2+}/Mg^{2+} supplemented with 2%
434 FBS and 2 mM EDTA) containing a mix of antibodies for 30 min at 4°C. The following antibodies
435 were purchased from BioLegend if not indicated otherwise: anti-mouse CD45 (clone 30-F11),
436 anti-mouse/human CD45R/B220 (clone RA3-6B2), anti-mouse GL7 (clone GL7), anti-mouse
437 CD4 (clone GK1.5), anti-mouse IgA (eBioscience, clone mA-6E1). For the staining of IgA^+ cells,
438 both surface and intracellular staining were performed. Multi-parameter analysis was conducted
439 with BD™ LSR II flow cytometry and analyzed with FlowJo software (Tree Star, Inc.). Only live
440 cells and singlets were used in all analyses (Supplementary Fig. 9).
441
442 **Extraction of bacterial DNA from feces**
443 Each murine fecal pellet was collected into a 2 ml screw cap tube (Axygen Scientific,
444 SCT200SSC) and stored at -80°C freezer until processing. Each sample was mixed with 1.3 ml
445 of buffer, composed of 282 µl of DNA buffer A (20 mM Tris pH 8.0, 2 mM EDTA and 200 mM
446 NaCl), 200 µl of 20% SDS (v/w), 550 µl of Phenol:Chloroform:IAA (25:24:1) (Ambion, AM9732)
447 and 268 µl of Buffer PM (Qiagen, 19083), and 400 µl of 0.1 mm diameter zirconia/silica beads
448 (BioSpec, 11079101z). Next, the sample was mechanically lysed with a Mini-Beadbeater-96
449 (BioSpec, 1001) for 5 min at room temperature. After centrifuging for 5 min at 4000 rpm
450 (Eppendorf Centrifuge 5810 R), all aqueous phase was collected, mixed with 650 µl of Buffer

451 PM thoroughly before running through a Qiagen spin column. The column was washed twice
452 with Buffer PE (Qiagen, 19065). Attached DNA was eluted with 100 µl of Buffer EB (Qiagen,
453 19086) and quantified with Qubit™ dsDNA Assay Kit (Thermo Fisher Scientific,
454 Q32853/Q32854). Bacteria density was calculated by the following equation: Bacteria Density =
455 DNA yield per sample (ug) / weight of sample (mg)[66].
456
457 **Bacterial genome and metagenomic sequencing**
458 Purified bacterial template DNA (~250 ng) was sonicated and prepared using the NEBNext®
459 Ultra™ II DNA Library Prep kit. Samples were pooled and sequenced with an Illumina HiSeq
460 4000 with pair-end 150nt reads. Metagenomic sequencing reads were mapped back to the
461 reference genomes for each experiment to determine the relative abundance of each strain. To
462 uniquely distinguish each strain, 100K sequencing reads for each sample were mapped to the
463 unique regions of each genome and final abundances were scaled by the unique genome size
464 of each strain (i.e. genome equivalents), as previously described[67].
465
466 **Immunofluorescence staining**
467 Immunofluorescence staining was performed as described previously[25,60]. Briefly, intestinal
468 tissues were fixed in 10% neutral formalin overnight at 4°C, dehydrated in 15% and 30%
469 sucrose buffer sequentially and mounted in O.C.T Embedding Compound (Electron Microscopy
470 Sciences). Cryostat sections (~8 µm) were prepared, blocked with anti-CD16/32 antibody in
471 10% (v/v) rat serum/0.1% Triton-X100 in PBS for 30 min at room temperature and incubated
472 with the indicated primary antibodies at 4°C overnight. The following primary antibodies were
473 used: rat anti-mouse IgA-FITC (1/300 dilution; eBioscience, clone mA-6E1), goat anti-mouse
474 pIgR (1/500 dilution; R&D Systems, cat #: AF2800). Slides were washed in PBS for three times,
475 incubated with Alexa Fluor®-conjugated species-specific secondary antibody (1/400 dilution;
476 Invitrogen) for 1 h at room temperature if needed and finally mounted with ProLong® Gold Anti-

477 fade Reagent with DAPI (Invitrogen). Fluorescence images of sections were acquired with a
478 LSM780 confocal laser-scanning microscope (Carl Zeiss) and further processed in ImageJ if
479 necessary.
480
481 **Statistical analysis**
482 Data are shown as mean ± SEM. Statistical significance between two groups was assessed by
483 an unpaired, two-tailed Student's *t* test. Comparisons among three or more groups were
484 performed using One-way ANOVA. Bimodality distribution of IgA levels induced by different *B.*
485 *ovatus* strains was performed in R (R package 'diptest'). For correlation test, Pearson
486 correlation coefficient was employed. Data plotting, interpolation and statistical analysis were
487 performed using GraphPad Prism 6.0 (GraphPad Software, La Jolla, CA) or R statistical
488 software (version 3.2.2). A *p*-value less than 0.05 is considered statistically significant.
489

490 **Data availability**

491 Bacterial genomes and metagenomic sequencing reads for this study are available via NCBI
492 BioProject accession number PRJNA518912.

493

494 **Acknowledgments**

495 We are grateful to C. Fermin, E. Vazquez, and G. Escano for the husbandry of gnotobiotic mice;
496 Drs. Anuk Das, Dirk Gevers, C. Cunningham-Rundles, B. Brown and T. Moran for helpful
497 discussions and comments. This work was supported in part by the staff and resources of the
498 Gnotobiotic Mouse Core Facility, the Microbiome Translational Center, the Flow Cytometry Core
499 Facility and the Scientific Computing Division in Icahn School of Medicine at Mount Sinai. This
500 work was supported by National Institutes of Health Grants (NIGMS GM108505 and NCCIH
501 AT008661) and Janssen Human Microbiome Institute (to J.J.F.) and NIH DK112679 (to E.J.C.).

502

503 **Author contributions**

504 C.Y. and J.J.F conceived the study and designed the experiments; C.Y., I.M., E.J.C., J.B., V.A.,
505 E.G., D.H., M.D. and J.J.F. collected samples and conducted the experiments; I.M. and Z.L.
506 provided bacterial isolates; C.Y., S.M., A.C. and J.J.F. analyzed data; C.Y. and J.J.F. prepared
507 the manuscript. All authors read and approved the final manuscript.

508

509 **Competing interests**

510 J.J.F. serves as a consultant for Janssen Research & Development LLC. The other authors
511 declare no conflict of interests.

512

References

1 Sutherland, D. B., Suzuki, K. & Fagarasan, S. Fostering of advanced mutualism with gut microbiota by Immunoglobulin A. *Immunological Reviews* **270**, 20-31, doi:10.1111/imr.12384 (2016).

2 Cerutti, A. & Rescigno, M. The biology of intestinal immunoglobulin A responses. *Immunity* **28**, 740-750, doi:10.1016/j.immuni.2008.05.001 (2008).

3 Macpherson, A. J., Geuking, M. B. & McCoy, K. D. Homeland Security: IgA immunity at the frontiers of the body. *Trends Immunol* **33**, 160-167, doi:10.1016/j.it.2012.02.002 (2012).

4 Okai, S. *et al.* High-affinity monoclonal IgA regulates gut microbiota and prevents colitis in mice. *Nat Microbiol* **1**, 16103, doi:10.1038/nmicrobiol.2016.103 (2016).

5 Tokuhara, D. *et al.* Secretory IgA-mediated protection against V. cholerae and heat-labile enterotoxin-producing enterotoxigenic Escherichia coli by rice-based vaccine. *Proc Natl Acad Sci U S A* **107**, 8794-8799, doi:10.1073/pnas.0914121107 (2010).

6 Strugnell, R. A. & Wijburg, O. L. C. The role of secretory antibodies in infection immunity. *Nat Rev Microbiol* **8**, 656-667, doi:10.1038/nrmicro2384 (2010).

7 Fagarasan, S. Evolution, development, mechanism and function of IgA in the gut. *Curr Opin Immunol* **20**, 170-177, doi:10.1016/j.coi.2008.04.002 (2008).

8 Pabst, O. New concepts in the generation and functions of IgA. *Nature Reviews Immunology* **12**, 821-832, doi:10.1038/nri3322 (2012).

9 McLoughlin, K., Schluter, J., Rakoff-Nahoum, S., Smith, A. L. & Foster, K. R. Host Selection of Microbiota via Differential Adhesion. *Cell Host Microbe* **19**, 550-559, doi:10.1016/j.chom.2016.02.021 (2016).

10 Donaldson, G. P. *et al.* Gut microbiota utilize immunoglobulin A for mucosal colonization. *Science* **360**, 795-800, doi:10.1126/science.aaq0926 (2018).

11 Viladomiu, M. *et al.* IgA-coated E. coli enriched in Crohn's disease spondyloarthritis promote TH17-dependent inflammation. *Sci Transl Med* **9**, doi:10.1126/scitranslmed.aaf9655 (2017).

12 Palm, N. W. *et al.* Immunoglobulin A coating identifies colitogenic bacteria in inflammatory bowel disease. *Cell* **158**, 1000-1010, doi:10.1016/j.cell.2014.08.006 (2014).

13 Kau, A. L. *et al.* Functional characterization of IgA-targeted bacterial taxa from undernourished Malawian children that produce diet-dependent enteropathy. *Sci Transl Med* **7**, 276ra224, doi:10.1126/scitranslmed.aaa4877 (2015).

14 Macpherson, A. J. *et al.* A primitive T cell-independent mechanism of intestinal mucosal IgA responses to commensal bacteria. *Science* **288**, 2222-+, doi:DOI 10.1126/science.288.5474.2222 (2000).

15 Hapfelmeier, S. *et al.* Reversible microbial colonization of germ-free mice reveals the dynamics of IgA immune responses. *Science* **328**, 1705-1709, doi:10.1126/science.1188454 (2010).

16 Peterson, D. A., McNulty, N. P., Guruge, J. L. & Gordon, J. I. IgA response to symbiotic bacteria as a mediator of gut homeostasis. *Cell Host Microbe* **2**, 328-339, doi:10.1016/j.chom.2007.09.013 (2007).

17 Fritz, J. H. *et al.* Acquisition of a multifunctional IgA+ plasma cell phenotype in the gut. *Nature* **481**, 199-203, doi:10.1038/nature10698 (2011).

18 Macpherson, A. J., McCoy, K. D., Johansen, F. E. & Brandtzaeg, P. The immune geography of IgA induction and function. *Mucosal Immunol* **1**, 11-22, doi:10.1038/mi.2007.6 (2008).

19 Bunker, J. J. *et al.* Innate and Adaptive Humoral Responses Coat Distinct Commensal Bacteria with Immunoglobulin A. *Immunity* **43**, 541-553, doi:10.1016/j.immuni.2015.08.007 (2015).

563 20 Lindner, C. *et al.* Diversification of memory B cells drives the continuous adaptation of
564 secretory antibodies to gut microbiota. *Nat Immunol* **16**, 880-888, doi:10.1038/ni.3213
565 (2015).
566 21 Obata, T. *et al.* Indigenous opportunistic bacteria inhabit mammalian gut-associated
567 lymphoid tissues and share a mucosal antibody-mediated symbiosis. *P Natl Acad Sci*
568 *USA* **107**, 7419-7424, doi:10.1073/pnas.1001061107 (2010).
569 22 Lecuyer, E. *et al.* Segmented filamentous bacterium uses secondary and tertiary
570 lymphoid tissues to induce gut IgA and specific T helper 17 cell responses. *Immunity* **40**,
571 608-620, doi:10.1016/j.immuni.2014.03.009 (2014).
572 23 Chudnovskiy, A. *et al.* Host-Protozoan Interactions Protect from Mucosal Infections
573 through Activation of the Inflammasome. *Cell* **167**, 444-456 e414,
574 doi:10.1016/j.cell.2016.08.076 (2016).
575 24 Shibata, N. *et al.* Lymphoid tissue-resident Alcaligenes LPS induces IgA production
576 without excessive inflammatory responses via weak TLR4 agonist activity. *Mucosal*
577 *Immunol*, doi:10.1038/mi.2017.103 (2018).
578 25 Moon, C. *et al.* Vertically transmitted faecal IgA levels determine extra-chromosomal
579 phenotypic variation. *Nature* **521**, 90-93, doi:10.1038/nature14139 (2015).
580 26 Macpherson, A. J., Koller, Y. & McCoy, K. D. The bilateral responsiveness between
581 intestinal microbes and IgA. *Trends Immunol* **36**, 460-470, doi:10.1016/j.it.2015.06.006
582 (2015).
583 27 Faith, J. J., Ahern, P. P., Ridaura, V. K., Cheng, J. & Gordon, J. I. Identifying gut
584 microbe-host phenotype relationships using combinatorial communities in gnotobiotic
585 mice. *Sci Transl Med* **6**, 220ra211, doi:10.1126/scitranslmed.3008051 (2014).
586 28 Atarashi, K. *et al.* Induction of colonic regulatory T cells by indigenous Clostridium
587 species. *Science* **331**, 337-341, doi:10.1126/science.1198469 (2011).
588 29 Round, J. L. & Mazmanian, S. K. Inducible Foxp3+ regulatory T-cell development by a
589 commensal bacterium of the intestinal microbiota. *Proc Natl Acad Sci U S A* **107**, 12204-
590 12209, doi:10.1073/pnas.0909122107 (2010).
591 30 Ivanov, II *et al.* Induction of intestinal Th17 cells by segmented filamentous bacteria. *Cell*
592 **139**, 485-498, doi:10.1016/j.cell.2009.09.033 (2009).
593 31 Mortha, A. *et al.* Microbiota-dependent crosstalk between macrophages and ILC3
594 promotes intestinal homeostasis. *Science* **343**, 1249288, doi:10.1126/science.1249288
595 (2014).
596 32 Britton, G. J. *et al.* Microbiotas from Humans with Inflammatory Bowel Disease Alter the
597 Balance of Gut Th17 and RORgammat(+) Regulatory T Cells and Exacerbate Colitis in
598 Mice. *Immunity* **50**, 212-224 e214, doi:10.1016/j.immuni.2018.12.015 (2019).
599 33 Clemente, J. C., Manasson, J. & Scher, J. U. The role of the gut microbiome in systemic
600 inflammatory disease. *BMJ* **360**, j5145, doi:10.1136/bmj.j5145 (2018).
601 34 Smillie, C. S. *et al.* Strain Tracking Reveals the Determinants of Bacterial Engraftment in
602 the Human Gut Following Fecal Microbiota Transplantation. *Cell Host Microbe* **23**, 229-
603 240 e225, doi:10.1016/j.chom.2018.01.003 (2018).
604 35 Seekatz, A. M. *et al.* Recovery of the gut microbiome following fecal microbiota
605 transplantation. *MBio* **5**, e00893-00814, doi:10.1128/mBio.00893-14 (2014).
606 36 Shankar, V. *et al.* Species and genus level resolution analysis of gut microbiota in
607 Clostridium difficile patients following fecal microbiota transplantation. *Microbiome* **2**, 13,
608 doi:10.1186/2049-2618-2-13 (2014).
609 37 Clemente, J. C. & Dominguez-Bello, M. G. Safety of vaginal microbial transfer in infants
610 delivered by caesarean, and expected health outcomes. *BMJ* **352**, i1707,
611 doi:10.1136/bmj.i1707 (2016).

612 38 Petrof, E. O. & Khoruts, A. From stool transplants to next-generation microbiota
613 therapeutics. *Gastroenterology* **146**, 1573-1582, doi:10.1053/j.gastro.2014.01.004
614 (2014).
615 39 Human Microbiome Project, C. Structure, function and diversity of the healthy human
616 microbiome. *Nature* **486**, 207-214, doi:10.1038/nature11234 (2012).
617 40 Turnbaugh, P. J. *et al.* A core gut microbiome in obese and lean twins. *Nature* **457**, 480-
618 484, doi:10.1038/nature07540 (2009).
619 41 Kanasugi, H. *et al.* Single administration of enterococcal preparation (FK-23) augments
620 non-specific immune responses in healthy dogs. *Int J Immunopharmacol* **19**, 655-659
621 (1997).
622 42 Reber, S. O. *et al.* Immunization with a heat-killed preparation of the environmental
623 bacterium Mycobacterium vaccae promotes stress resilience in mice. *Proc Natl Acad Sci*
624 *U S A* **113**, E3130-3139, doi:10.1073/pnas.1600324113 (2016).
625 43 Faith, J. J. *et al.* The long-term stability of the human gut microbiota. *Science* **341**,
626 1237439, doi:10.1126/science.1237439 (2013).
627 44 Faith, J. J., Colombel, J.-F. & Gordon, J. I. Identifying strains that contribute to complex
628 diseases through the study of microbial inheritance. *Proceedings of the National*
629 *Academy of Sciences* **112**, 633-640, doi:10.1073/pnas.1418781112 (2015).
630 45 Shijie Zhao, T. D. L., Mathilde poyet, Sean M. Gibbons, Mathieu Groussin, Ramnik J.
631 Xavier, Eric J. Alm. Adaptive evolution within the gut microbiome of individual people.
632 *BioRxiv*, doi:https://doi.org/10.1101/208009 (2018).
633 46 Vatanen, T. *et al.* Genomic variation and strain-specific functional adaptation in the
634 human gut microbiome during early life. *Nat Microbiol*, doi:10.1038/s41564-018-0321-5
635 (2018).
636 47 Kim, M., Qie, Y., Park, J. & Kim, C. H. Gut Microbial Metabolites Fuel Host Antibody
637 Responses. *Cell Host Microbe* **20**, 202-214, doi:10.1016/j.chom.2016.07.001 (2016).
638 48 Fransen, F. *et al.* BALB/c and C57BL/6 Mice Differ in Polyreactive IgA Abundance,
639 which Impacts the Generation of Antigen-Specific IgA and Microbiota Diversity. *Immunity*
640 **43**, 527-540, doi:10.1016/j.immuni.2015.08.011 (2015).
641 49 Johansen, F. E. & Kaetzel, C. S. Regulation of the polymeric immunoglobulin receptor
642 and IgA transport: new advances in environmental factors that stimulate pIgR expression
643 and its role in mucosal immunity. *Mucosal Immunol* **4**, 598-602, doi:10.1038/mi.2011.37
644 (2011).
645 50 Hooper, L. V. *et al.* Molecular analysis of commensal host-microbial relationships in the
646 intestine. *Science* **291**, 881-884, doi:10.1126/science.291.5505.881 (2001).
647 51 Schneeman, T. A. *et al.* Regulation of the Polymeric Ig Receptor by Signaling through
648 TLRs 3 and 4: Linking Innate and Adaptive Immune Responses. *The Journal of*
649 *Immunology* **175**, 376-384, doi:10.4049/jimmunol.175.1.376 (2005).
650 52 Chorny, A., Puga, I. & Cerutti, A. Innate Signaling Networks in Mucosal IgA Class
651 Switching. *Adv Immunol* **107**, 31-69, doi:10.1016/S0065-2776(10)07006-9 (2010).
652 53 Suzuki, K., Kawamoto, S., Maruya, M. & Fagarasan, S. GALT: Organization and
653 Dynamics Leading to IgA Synthesis. *Adv Immunol* **107**, 153-185, doi:10.1016/S0065-
654 277600)07003-3 (2010).
655 54 Fagarasan, S., Kawamoto, S., Kanagawa, O. & Suzuki, K. Adaptive immune regulation
656 in the gut: T cell-dependent and T cell-independent IgA synthesis. *Annu Rev Immunol*
657 **28**, 243-273, doi:10.1146/annurev-immunol-030409-101314 (2010).
658 55 Palmela, C. *et al.* Adherent-invasive Escherichia coli in inflammatory bowel disease. *Gut*
659 **67**, 574-587, doi:10.1136/gutjnl-2017-314903 (2018).
660 56 Arthur, J. C. *et al.* Intestinal inflammation targets cancer-inducing activity of the
661 microbiota. *Science* **338**, 120-123, doi:10.1126/science.1224820 (2012).

57 Masahata, K. *et al.* Generation of colonic IgA-secreting cells in the caecal patch. *Nat Commun* **5**, 3704, doi:10.1038/ncomms4704 (2014).

58 Wang, Y. *et al.* An LGG-derived protein promotes IgA production through upregulation of APRIL expression in intestinal epithelial cells. *Mucosal Immunol* **10**, 373-384, doi:10.1038/mi.2016.57 (2017).

59 Kawamoto, S. *et al.* Foxp3(+) T cells regulate immunoglobulin a selection and facilitate diversification of bacterial species responsible for immune homeostasis. *Immunity* **41**, 152-165, doi:10.1016/j.immuni.2014.05.016 (2014).

60 Kunisawa, J. *et al.* Microbe-dependent CD11b+ IgA+ plasma cells mediate robust early-phase intestinal IgA responses in mice. *Nat Commun* **4**, 1772, doi:10.1038/ncomms2718 (2013).

61 van Nood, E. *et al.* Duodenal infusion of donor feces for recurrent Clostridium difficile. *N Engl J Med* **368**, 407-415, doi:10.1056/NEJMoa1205037 (2013).

62 Moayyedi, P. *et al.* Fecal Microbiota Transplantation Induces Remission in Patients With Active Ulcerative Colitis in a Randomized Controlled Trial. *Gastroenterology* **149**, 102-+, doi:10.1053/j.gastro.2015.04.001 (2015).

63 Rossen, N. G. *et al.* Findings From a Randomized Controlled Trial of Fecal Transplantation for Patients With Ulcerative Colitis. *Gastroenterology* **149**, 110-118 e114, doi:10.1053/j.gastro.2015.03.045 (2015).

64 Grinspan, A. M. & Kelly, C. R. Fecal Microbiota Transplantation for Ulcerative Colitis: Not Just Yet. *Gastroenterology* **149**, 15-18, doi:10.1053/j.gastro.2015.05.030 (2015).

65 Kruisbeek, A. M. In vivo depletion of CD4- and CD8-specific T cells. *Curr Protoc Immunol* **Chapter 4**, Unit 4 1, doi:10.1002/0471142735.im0401s01 (2001).

66 Contijoch, E. J. *et al.* Gut microbiota density influences host physiology and is shaped by host and microbial factors. *Elife* **8**, doi:10.7554/eLife.40553 (2019).

67 McNulty, N. P., Wu, M., Erickson, A. R., Pan, C. & Erickson, B. K. Effects of Diet on Resource Utilization by a Model Human Gut Microbiota Containing Bacteroides cellulosilyticus WH2, a Symbiont with an Extensive Glycobiome. *PLoS biology* **11**, e1001637, doi:10.1371/journal.pbio.1001637 (2013).

693 **Figures**

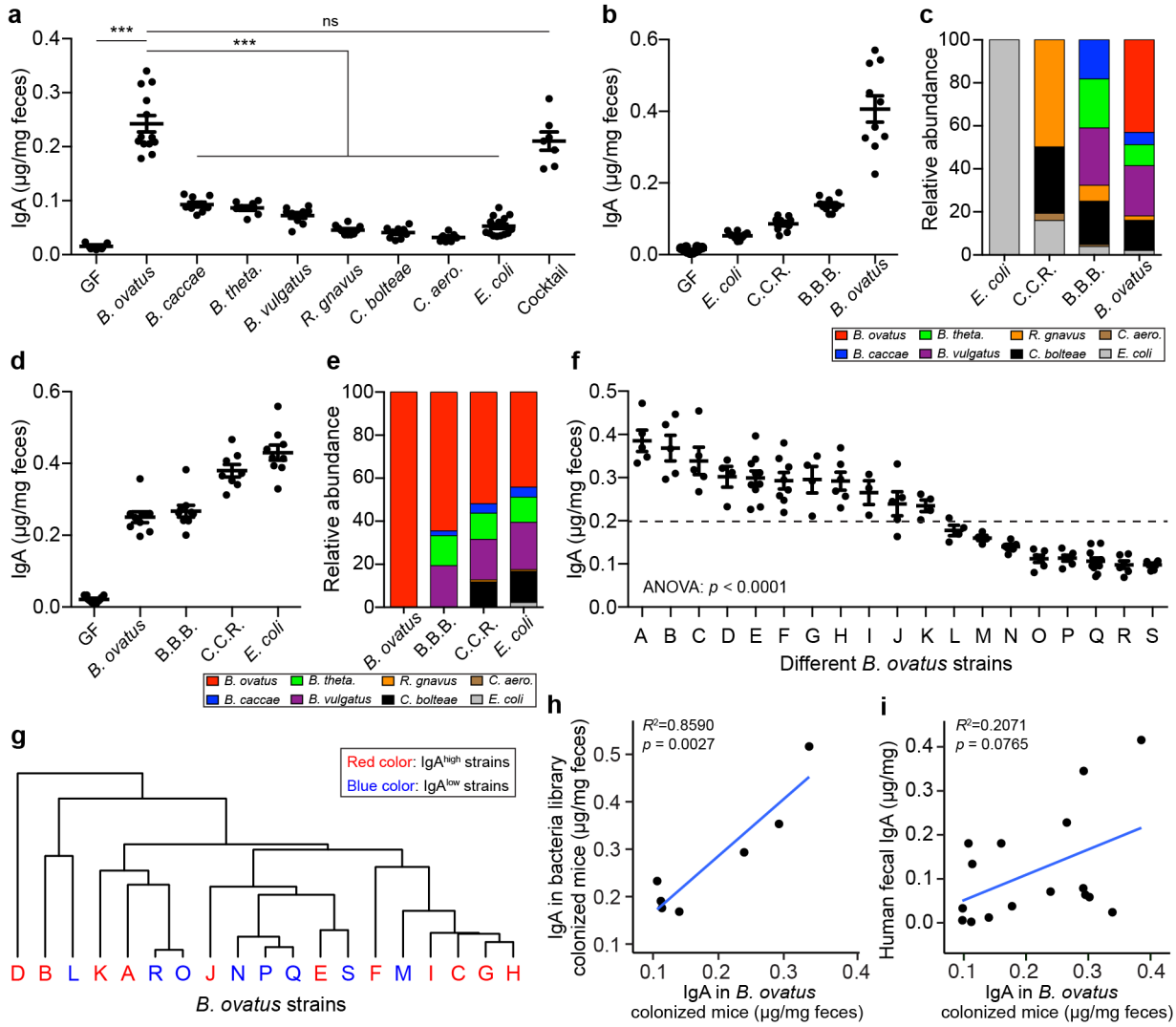

694

695 **Fig. 1 | *B. ovatus* species, with strain-level differences, predominantly induces fecal IgA**
696 **production in gnotobiotic mice.** (**a**) Fecal IgA level in C57BL/6 gnotobiotic mice colonized
697 with individual or a cocktail of human gut commensal bacteria for three weeks. (**b**-**e**) The
698 concentration of fecal IgA (**b** and **d**) and proportion of each bacterial strain (**c** and **e**) in stool of
699 gnotobiotic mice that were colonized sequentially with individual or combined bacterial
700 communities starting from *E. coli* (**b** and **c**) or *B. ovatus* (**d** and **e**). Feces were harvested before
701 addition of new bacteria to the same mice. C.C.R.: cocktail of *C. bolteae, C. aerofaciens* and *R.*
702 *gnavus*; B.B.B.: cocktail of *B. caccae, B. theta.* and *B. vulgatus* (**f**) Quantification of fecal IgA in

703 gnotobiotic mice upon colonization with an individual strain of *B. ovatus* for three weeks. Unique
704 strains of *B. ovatus* were isolated from the stools of different human donors. Dotted line
705 separates high- and low-IgA phenotypes. (**g**) Dendrogram clustering of different *B. ovatus*
706 strains basing on the dissimilarity of bacterial genomic DNA sequences. (**h**) Correlation of stool
707 IgA levels between single *B. ovatus* strain monocolonized mice versus mice colonized with a
708 microbiota arrayed culture collection that included that single *B. ovatus* strain. Both single *B.*
709 *ovatus* strains and arrayed culture collections were isolated from the same donor. (**i**) Correlation
710 of fecal IgA concentration between single *B. ovatus* strain colonized mice versus human donor.
711 Data shown are mean ± standard error of the mean. Each dot in **a**, **b**, **d** and **f** represents a
712 biological replicate. The average fecal IgA concentration from 4-10 mice was used for
713 correlation in **h** and **i**. Detailed strain information is listed in Supplementary Tables 1 and 2. *p*-
714 values with statistical significance (assessed by two-tailed Student's *t* test or one-way ANOVA)
715 are indicated: ***$p < 0.001$; ns, not significant.
716

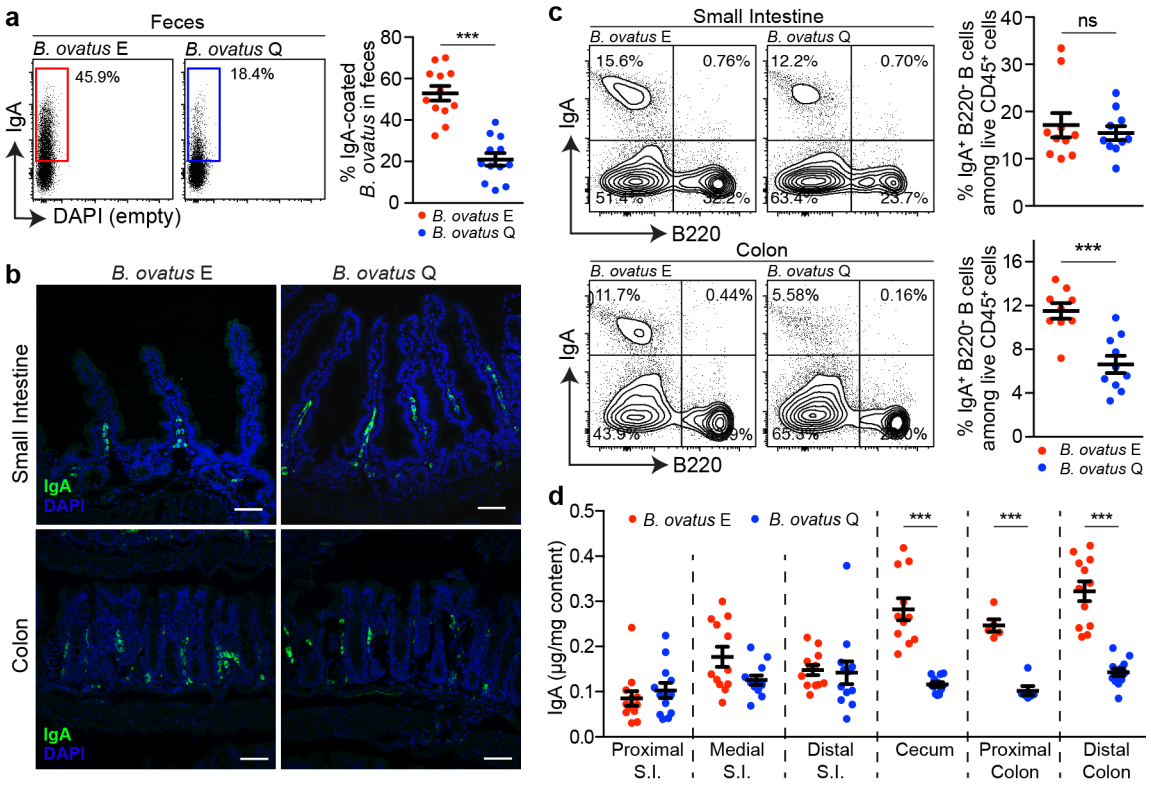

Fig. 2 | IgA^{high} *B. ovatus* strain elicits stronger IgA responses in the large intestine. (**a**) Representative flow cytometry plot and quantification of IgA-coated *B. ovatus* in feces of gnotobiotic mice harboring either *B. ovatus* strain *E* or *Q*. (**b**) Representative images of IgA^{+} cells in small intestine and the colon are shown. IgA^{+} cells were stained with anti-IgA (green); Nuclei were counter-stained with DAPI (4',6-diamidino-2-phenylindole) (blue). n = 5~6. Scale bar = 50 μm. (**c**) Percentage of IgA^{+} B cells in small intestinal and colonic tissues is shown. LP lymphocytes were analyzed by flow cytometry. Number adjacent to gate represents percentage. (**d**) Free IgA concentration in luminal contents along the length of the intestine. S.I.: small intestine. Data shown are mean ± standard error of the mean. Each dot represents an individual mouse. *p*-values with statistical significance (assessed by two-tailed Student's *t* test) are indicated: ***$p < 0.001$; ns, not significant.

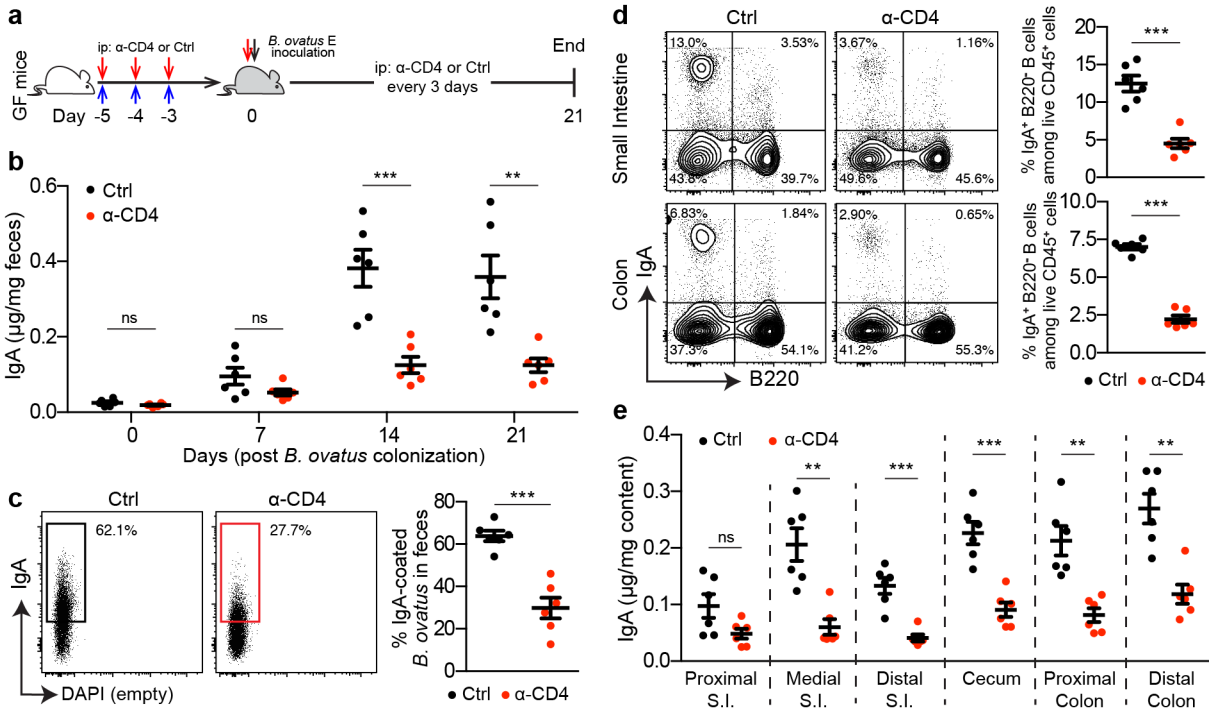

730

731 **Fig. 3 | Both T-cell-dependent and T-cell-independent pathways are involved in fecal IgA**
732 **induction mediated by *B. ovatus* strain *E*.** (**a**) Schematic representation of CD4$^+$ T cells
733 depletion in GF B6 mice is illustrated. Red arrows represent i.p. injection of anti-CD4 antibody or
734 isotype control. Black arrow indicates *B. ovatus* strain *E* inoculation and blue arrows represent
735 time. (**b**) Dynamics of fecal IgA concentration in *B. ovatus* strain *E* inoculated gnotobiotic B6
736 mice treated with either anti-CD4 antibody or isotype control. (**c**) Representative flow cytometry
737 plot and quantification of IgA-coated bacteria in feces of *B. ovatus* strain-*E*-colonized gnotobiotic
738 mice treated with either anti-CD4 antibody or isotype control. (**d**) Representative flow cytometry
739 plot and percentage of IgA$^+$ B cells in small intestine and the colon are shown. Numbers
740 adjacent to gates represent percentage. (**e**) Concentration of free IgA in the intestinal content
741 collected from different regions of the whole intestinal tract is shown. S.I.: small intestine. Data
742 shown are mean ± standard error of the mean. Each dot represents an individual mouse. *p*-
743 values with statistical significance (assessed by two-tailed Student's *t* test) are indicated: $^{**}p <$
744 0.01, $^{***}p < 0.001$; ns, not significant.

745

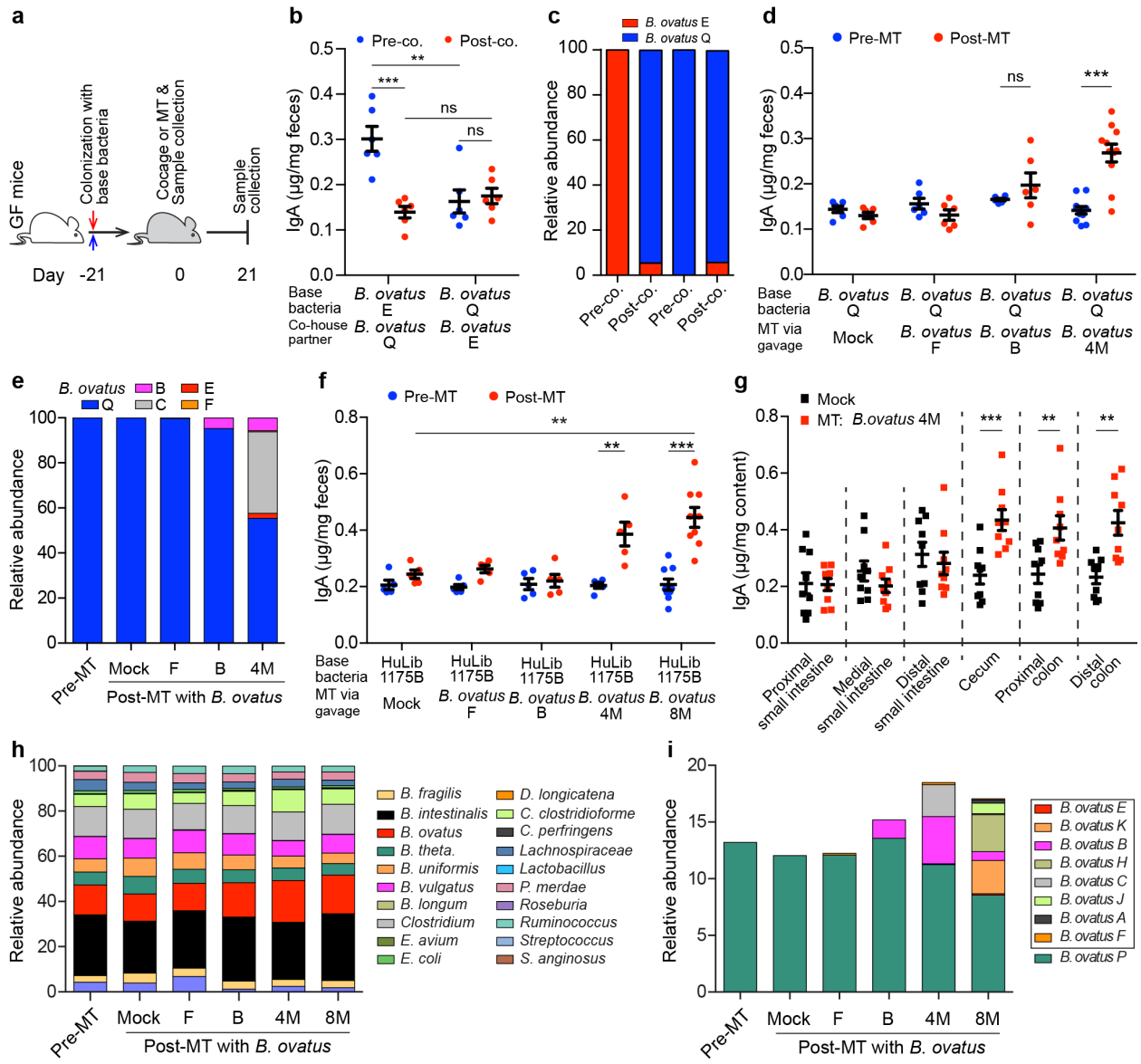

Fig. 4 | Multiplex microbial strains robustly transfer high-IgA phenotype to low-IgA producing mice. (**a**) Schematic representation of cohousing and microbial therapeutic strategies. (**b** and **c**) Fecal IgA concentration (**b**) and relative abundance of each *B. ovatus* strain (**c**) in pre- and post-cohoused gnotobiotic mice, which were pre-colonized with either *B. ovatus* strain *E* or *Q*. (**d** and **e**) Fecal IgA concentration (**d**) and relative abundance of each *B. ovatus* strain (**e**) in mice pre- and post-microbiota-based therapeutic (MT). Mice were first colonized with *B. ovatus* strain *Q* for three weeks and subsequently administered a microbial therapeutic comprised of either an individual IgA^{high} *B. ovatus* strain or a cocktail of IgA^{high} *B.*

755 *ovatus* strains. (**f**) Fecal IgA concentration in mice pre- and post-MT, which were pre-colonized
756 with human microbiota arrayed culture collection (e.g. HuLib1175B) for three weeks. The
757 therapeutic was either an individual IgA^{high} *B. ovatus* strain or a cocktail of IgA^{high} *B. ovatus*
758 strains. *B. ovatus* 4M: a cocktail of 4 different IgA^{high} *B. ovatus* strains; *B. ovatus* 8M: a cocktail
759 of 8 different IgA^{high} *B. ovatus* strains. (**g**) Free IgA concentration along the intestinal tract of
760 mice after gavage with Mock or *B. ovatus* 4M. (**h**) Relative abundance of bacterial species in
761 mice pre- and post-MT. (**i**) Relative abundance of different *B. ovatus* strains in mice pre- and
762 post-MT. Data shown are mean ± standard error of the mean. Sequencing plots display the
763 average abundance from five mice. Each dot represents a biological replicate. Detailed strain
764 information is listed in Supplementary Tables 2 and 6. *p*-values with statistical significance
765 (assessed by two-tailed Student's *t* test) are indicated: $^{**}p < 0.01$, $^{***}p < 0.001$; ns, not
766 significant.
767